

HAROLD J. HOGE
SUZANNE S. EICHACKER
DAVID L. FISKE
Quartermaster Research and
Engineering Center, Natick, Mass.

Studies of Jet Compression—I

Apparatus and Methods. Results With Air at Room Temperature

An experimental jet compressor (ejector) employing gases at subatmospheric pressures is described and data are presented showing efficiencies obtained with air used as both the driving and the driven fluid. A technique is described by means of which efficiency may be determined as a function of outlet pressure and entrainment ratio. Curves are presented showing that efficiency passes through a maximum as outlet pressure is increased. The compression ratio of the driven fluid likewise passes through a maximum as the outlet pressure is increased, but the maximum of efficiency occurs at a slightly higher pressure than the maximum of compression ratio. The highest efficiency achieved was 20.6 per cent, at an entrainment ratio of 1.3 and a compression ratio of 1.14. The ratio of pressure of driven stream to pressure of driving stream at time of contact has been determined. The value of this pressure ratio corresponding to maximum efficiency was found to increase linearly with entrainment ratio, over most of the range of the measurements.

Introduction

THE SIMPLICITY of jet compression makes it attractive for many applications from an engineering standpoint. In spite of the low efficiencies ordinarily achieved, jet compression has been rather widely employed in steam-jet refrigeration, in air ejectors, in mine and tunnel ventilation, in mercury diffusion pumps, etc. If higher efficiencies could be achieved, a number of practical uses for jet compression would be opened up, particularly in applications to refrigerators, heat pumps, and fluid circulators. The present paper is the first report on a program to determine to what extent the limitations on efficiency are fundamental, and to what extent efficiency can be improved by proper

geometrical design and by proper choice of operating conditions.

Experimental studies of jet compression have been made by Keenan, Neumann, and Lustwerk [1],¹ by Keenan and Neumann [2], by Kastner and Spooner [3], by Royds and Johnson [4], and by others. The results have been analyzed with the aid of basic thermodynamics and fluid mechanics, using the equations of energy, continuity, momentum, and state. Flügel [5] appears to have been the first to develop this type of analysis. These analyses contain simplifying assumptions such as "constant pressure mixing" or "constant area mixing," which have complicated the problem of comparing theory with experiment. The picture of the mixing process is not very clear, and in spite of the rather extensive published investigations of various sizes and shapes of nozzles, mixing throats, and diffusers, the design of jet pumps remains on a primarily empirical basis.

Contributed by the Hydraulic Division and presented at the Semi-Annual Meeting, Detroit, Mich., June 15-19, 1958, of THE AMERICAN SOCIETY OF MECHANICAL ENGINEERS.

NOTE: Statements and opinions advanced in papers are to be understood as individual expressions of their authors and not those of the Society. Manuscript received at ASME Headquarters, February 28, 1958. Paper No. 58-SA-13.

The present paper contains a description of our apparatus and of the method of taking and analyzing the data. It also contains the experimental results obtained with room-temperature air

¹ Numbers in brackets designate references at end of paper.

Nomenclature and Dimensions

- η = efficiency of the jet compressor, defined by equation (1)
- η_{MAX} = maximum efficiency attained for a fixed value of m/M
- m = flow of driven gas, lb per hr
- M = flow of driving gas, lb per hr
- P = pressure, mm Hg
- T = temperature, deg F abs
- h = enthalpy, Btu per lb
- s = entropy, Btu per lb deg F
- u = velocity, ft per sec
- c_p = specific heat at constant pressure, Btu per lb deg F
- G = flow per unit area, lb per hr ft²
- A = cross section area, ft²
- R = gas constant, 0.068549 Btu per lb air deg F abs

Superscripts:

* = state at sonic velocity

Subscripts:

- 1 = initial state of driving fluid
- 2 = state corresponding to isentropic expansion of driving fluid to pressure at state 5
- 3 = initial state of driven fluid
- 5 = state of driving fluid at beginning of mixing
- 6 = state of driven fluid at beginning of mixing
- 7 = state at completion of mixing
- 8 = final state, at compressor exit

9 = state corresponding to isentropic compression of driven fluid to pressure at final state 8

10 = state corresponding to isentropic expansion of driving fluid to pressure at final state 8

a, b, . . . i = taps for pressure measurement; refer to Fig. 2 for locations

The following dimensions refer to the apparatus used in the present experiments: Driving-fluid nozzle No. 2 (the only nozzle used):

(Continued on next page)

utilized as both the driving and the driven fluid. Only one driving-fluid nozzle (No. 2) was employed. The observed inlet and outlet pressures, together with the corresponding temperatures, have been used to compute the over-all efficiency of the jet compressor as influenced by the conditions of operation.

Apparatus and Procedure

A diagram of the apparatus is given in Fig. 1. Ordinary atmospheric air supplied both the driving and driven streams. The pressure difference motivating the jet is obtained by means of a large vacuum pump (15 cfm capacity) attached to the jet-compressor outlet. The use of lowered, as against elevated pressures, offers the advantage that all pressures are readily measured by mercury manometers. Reduced pressure offers also the advantage of reduced density, making possible a nozzle diameter of convenient size without excessive quantity of flow. Such a system makes it possible to use much higher pressure ratios than could be conveniently reached in a system in which atmospheric pressure is the low, rather than the high, limit.

The driving and driven streams are measured at atmospheric temperature and pressure by two ordinary (dry) gas meters. The two lines connecting the meters to the jet compressor each contain a simple needle valve (V_1 , V_2) to control the flow rate. The pressure drops across these two valves were always more than sufficient to produce sonic flow. Hence a valve could be adjusted to give a particular flow rate, which would remain constant except for the small changes due to variations in room temperature and barometric pressure. The nondependence of flow rate on downstream conditions proved to be a great convenience in taking data. The lines from the meters to the jet compressor passed through thermostated heating baths designed to control the stream temperatures. Thus far these baths have not been used.

Three thermocouples are placed inside the jet compressor, to measure, respectively, the inlet temperature of the driving and the driven streams, and the outlet temperature of the mixed stream. Temperature measurements were made with these couples on a few occasions, to see whether there was any net heat transfer from the apparatus to the gas flowing through it. In one case (run 70) the outlet temperature was about 2.5 deg F higher than the weighted average of the inlet temperatures, but mostly the changes were less than 1 deg F and are considered small enough to be neglected in the present paper.

The pressure at the outlet of the jet compressor is controlled by valve V_3 in the line leading to the vacuum pump. This valve consisted of a length of heavy-wall rubber tubing ($\frac{3}{8}$ inch ID) clamped between two boards that could be drawn together by screwing down on a hand wheel. Adjustment of the outlet pressure to any desired value required only a few seconds.

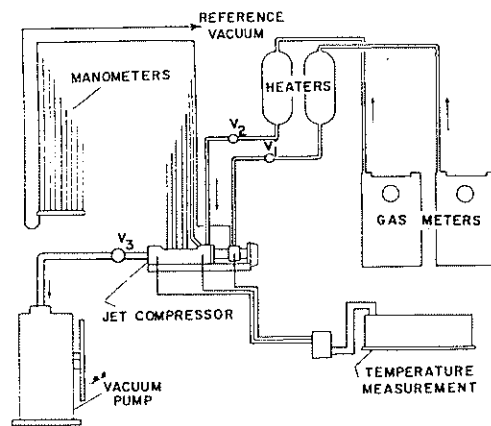


Fig. 1 Flow diagram of experimental equipment

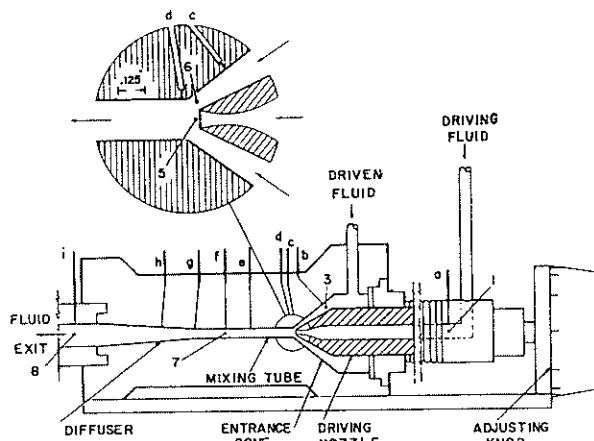


Fig. 2 Cross section of jet compressor with enlarged view of entrance to mixing tube

The central element of the experimental equipment is shown in Fig. 2. It is an assembly of brass parts composing an ejector system. The major part, indicated as "jet compressor" in Fig. 1, consists of entrance cone, mixing tube, and diffuser. The driving-fluid nozzle may be moved axially with respect to the rest of the apparatus. It is the function of the bellows to permit movement of the nozzle without loss of gas by leakage past the gland. Nozzle position is controlled by rotation of the adjusting knob, one

Nomenclature and Dimensions

throat diameter = 0.0595 in.
 exit diameter = 0.0710 in.
 throat-to-exit distance = 0.122 in.
 angle of outer conical surface with axis = 25 deg

Entrance cone for driven fluid:

diameter at upstream end = 1.25 in.
 angle of wall with axis = 35 deg

Mixing tube:

diameter = 0.1875 in.
 length = 1.67 in.
 length ÷ diameter = 8.9

Diffuser:

diameter at tap g = 0.1891 in.
 diameter at tap h = 0.2544 in.
 diameter at outlet = 0.3755 in.
 length = 1.80 in.
 angle of wall with axis = 3.0 deg

Distance of planes of pressure-tap openings, etc., from junction of entrance cone and mixing tube, measured along axis of flow, with distances increasing in direction of flow:

beginning of entrance cone = -0.76 in.

tap b = -0.48 in.
 tap c = -0.18 in.
 junction of entrance cone and mixing tube = 0 in.
 tap d = +0.03 in.
 tap e = 0.65 in.
 tap f = 1.15 in.
 junction of mixing tube and diffuser = 1.67 in.
 tap g = 1.69 in.
 tap h = 2.31 in.
 end of diffuser = 3.47 in.

graduation of which corresponds to a nozzle movement of 0.001 inch.

Provision is made for pressure measurements at 9 different points within the jet apparatus. The various pressure taps are lettered a, b, . . . i in the diagrams, and each is connected to an arm of a mercury manometer. Two mercury manometers are used, each with a reference arm in which a vacuum is maintained by a mercury-diffusion pump. The pressure readings are thus absolute.

When the flow of driven fluid is equal to or greater than the flow of driving fluid, the amount of compression produced is small. That is, the compression ratio is only slightly greater than unity. Under these conditions changes in pressure within the jet compressor could not be measured with sufficient accuracy with the mercury manometers. An oil manometer was therefore added, and was connected in parallel with the mercury manometer, to all taps except tap a, at which the pressures were too high to be read on the oil manometer. The oil manometer can be used either as a differential or as an absolute manometer. The ratio of the densities of mercury and oil, as determined by a comparison of column heights when both were relatively large, is 14.813. The use of the oil manometer appears to have increased the accuracy of the data at least tenfold in the regions where the mercury manometer was unsatisfactory.

Definition of Efficiency of Jet Compressor

The jet compressor receives two streams of fluid, one at a relatively high pressure and the other at a relatively low pressure,

and delivers them as a single stream at some intermediate pressure. Useful work is done in compressing the low-pressure stream, and the source of this work is the expansion of the high-pressure stream. The process may be conveniently followed by reference to the enthalpy-entropy diagram of Fig. 3. This is an actual representation of some of the experimental data plotted to scale, but our present concern is only with the qualitative aspects of the diagram. Point 1 represents the initial state of the driving fluid, and the condition line 1-5 represents states that are passed through during expansion and acceleration in the driving-fluid nozzle. The positions within the apparatus at which the various states are reached are shown in Fig. 2 by a series of points numbered to correspond to the points in Fig. 3. The points numbered 3 represent initial states of the driven fluid. For definiteness, consider only the one referring to observation 79k. The condition line 3-6 represents states along the path of expansion and acceleration of the driven fluid before it meets the driving fluid. The point 6 is enclosed in parentheses because, unlike the other points on the diagram, it is not plotted to scale. The mixing process cannot be represented on the diagram, but after mixing, the moving stream is in some state 7. The condition lines 7-8 represent states along the path of final deceleration and compression to the outlet pressure P_3 .

In the jet compression process, driving fluid has decreased in pressure from state 1 to the outlet pressure P_3 . If such a process were to occur in a lossless turbine the maximum work that could be performed by unit mass of driving fluid is equal to the isentropic enthalpy drop $h_1 - h_{1s}$. We will accept the same definition

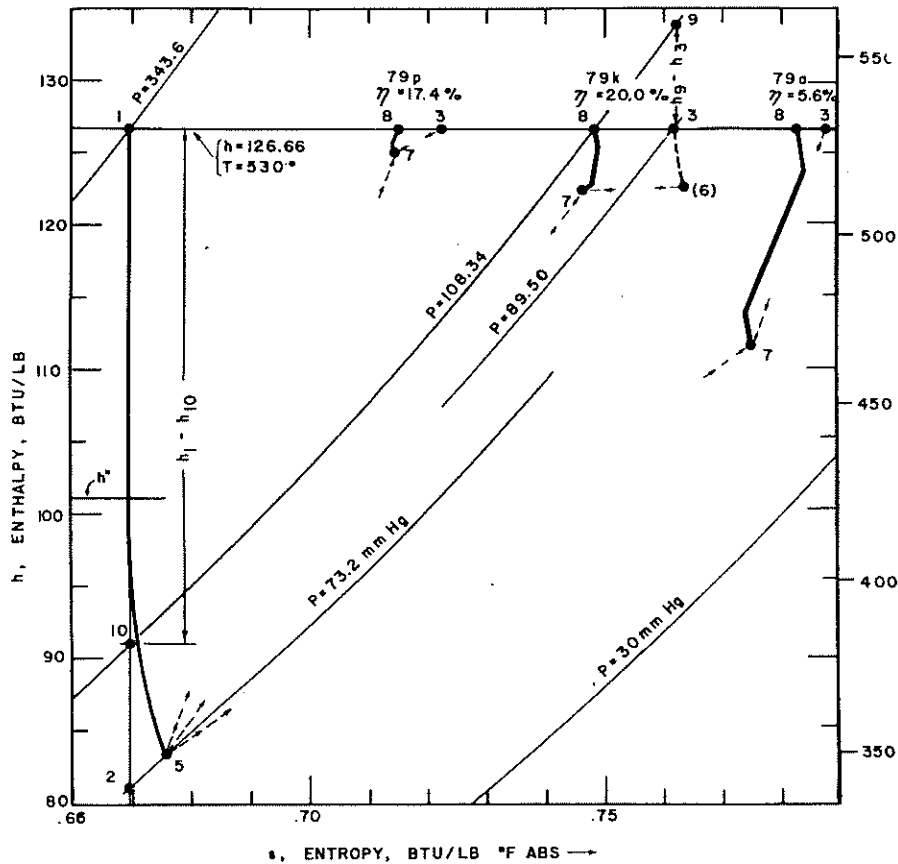


Fig. 3 Enthalpy-entropy diagram showing condition lines for observations 79a, 79k, and 79p. Drawn to scale except for point 6 which is schematic.

for the maximum work that could be done by unit mass of driving fluid in passing through a hypothetical lossless jet compressor. If we similarly imagine a lossless compressor compressing driven fluid from state 3 to the outlet pressure P_3 , the minimum work required per unit mass is equal to the isentropic enthalpy rise $h_3 - h_2$. We will accept $h_3 - h_2$ as the amount of work done when unit mass of driven fluid passes through the jet compressor. Let m be the rate of flow of driven fluid in pounds per hour, and let M be the corresponding rate of flow of the driving fluid. Then the work actually done within the apparatus in one second is $m(h_3 - h_2)$ and the maximum work that could be done in a lossless process is $M(h_1 - h_{10})$. The efficiency η is defined as the ratio of these quantities or

$$\eta = \frac{m}{M} \frac{h_3 - h_2}{h_1 - h_{10}} \quad (1)$$

In the actual jet-compression process the two streams are mixed and delivered in state 8, whereas in the idealized process used for comparison the turbine exhaust is in state 10 and the blower output is in state 9. It is recognized that states 9 and 10 are not in general "dead states." If point 8 represents the dead state, the temperature differences $T_9 - T_8$ and $T_{10} - T_8$ could be used to operate Carnot engines and perform work as the fluids were brought from states 9 and 10 to state 8. It is customary to disregard such quantities of work in defining the efficiency of a steam turbine [6], and it appears desirable to follow the same practice for jet compression, even though the quantities of work disregarded may be relatively more important in the jet compressor. If we were to include these quantities of work in the computation we would obtain a quantity based on changes in available energy that Keenan [6, p. 297] has called the effectiveness, to distinguish it from the conventional efficiency.

Having defined the efficiency η in the conventional manner, one must keep in mind that η refers to only one step in the complete process in which thermal energy is used to do useful work of compression. To obtain high over-all thermodynamic efficiency, we must first learn how to design a jet compressor giving a high value of η . Then such a compressor must be incorporated into a system that is thermodynamically efficient in the over-all sense. That is, heat must be absorbed at the highest practical temperature and rejected at the lowest practical temperature. All irreversible processes must be reduced in importance. The last condition requires that T_8 , T_9 , and T_{10} should not be widely different, and in part establishes the optimum location of state 1 relative to states 3 and 8.

Experimental Results

In a typical run, the mass rates of flow m and M were set to the desired values and held constant throughout the run. The outlet pressure P_3 was set at some desired value and the 9 pressures were read and recorded. Then P_3 was set at another value and the process repeated until the run was completed. In all the data now being reported, the position of the driving-fluid nozzle was held constant. The nozzle was advanced until it touched the entrance to the combining tube. It was then backed off 0.175 in. at which position the tip was 0.05 in. upstream from the entrance to the mixing tube. The circular insert in Fig. 2 is a scale drawing of the nozzle in operating position. All measurements reported here were taken with this setting. In several preliminary measurements, efficiency was measured as a function of nozzle position. These measurements indicated that, so long as extreme settings were avoided, the effect of nozzle position on efficiency was not large. The accepted setting is an intermediate one that is believed to be reasonably suitable for all the data reported. The observed volume rates of flow were converted to mass rates

Table 1 Experimental data for three typical runs

Observation	Pressures, mm Hg, at various taps									η	$\frac{m}{M}$
	a (P_1)	b (P_2)	c	d (P_6)	e	f (P_7)	g	h	i (P_3)		
	Run 64, $m/M = 0.0744$										
a	342.5	13.8	13.80	13.53	13.39	15.02	12.65	12.28	20.75	1.66	
n	339.5	13.5	13.47	13.10	15.02	18.16	21.80	33.42	37.67	5.43	
p	339.2	14.2	14.17	13.73	21.36	32.68	34.38	40.02	42.66	6.16	
c	341.5	15.0	16.30	15.46	28.12	37.60	38.79	42.85	44.21	6.02	
e	341.3	22.7	22.70	22.36	36.94	45.45	49.16	52.94	54.73	5.23	
	Run 47, $m/M = 0.421$										
a	341.0	34.0	34.00	33.59	48.99	61.34	62.22	65.19	66.61	4.22	
i	341.2	62.7	62.70	62.55	85.25	91.59	91.05	81.03	93.99	2.95	
t	342.0	140.0	140.00	139.53	161.60	164.10	153.29	164.64	165.21	1.92	
	Run 79, $m/M = 1.00$										
a	344.5	30.5	30.44	29.10	24.22	26.52	20.39	18.15	30.64	0.11	
k	343.8	30.5	30.43	29.30	25.91	28.34	27.09	34.99	42.48	9.36	
w	342.0	35.7	35.63	31.99	34.55	40.22	42.99	50.96	55.83	14.14	
d	344.2	44.9	44.83	42.47	45.37	52.39	59.08	66.30	69.61	15.38	
j	341.1	52.1	52.00	50.58	58.48	71.85	71.31	75.98	78.19	14.99	
	Run 84, $m/M = 0.0744$										
d	345.1	75.2	75.17	73.95	86.58	95.87	96.37	100.31	101.93	12.98	
i	344.2	108.6	108.57	107.72	128.11	130.71	129.76	132.23	133.48	10.79	
h	345.3	153.1	153.07	152.53	170.15	172.98	172.31	174.20	175.11	9.43	
g	344.5	180.0	179.66	179.53	198.20	197.96	197.35	198.97	199.85	8.26	
	Run 79, $m/M = 1.00$										
a	342.2	61.2	60.80	50.06	47.50	47.55	52.15	59.11	65.79	5.58	
b	342.6	65.6	65.25	56.01	54.60	55.96	61.96	68.85	74.44	10.40	
w	338.3	67.5	67.15	60.93	60.25	65.86	69.64	76.39	81.99	14.56	
d	337.2	72.5	72.16	64.33	64.10	71.22	74.73	81.95	87.08	16.61	
u	343.7	74.7	74.43	66.87	67.54	75.51	78.68	86.01	90.67	18.03	
	Run 79, $m/M = 1.00$										
r	343.4	75.1	75.10	68.84	69.29	78.70	81.40	88.69	93.01	18.58	
v	344.2	79.8	79.46	72.58	74.74	84.26	86.11	93.30	97.28	19.17	
g	344.8	84.0	83.66	77.12	81.29	89.91	91.53	98.45	102.19	19.60	
f	344.6	84.7	84.39	77.95	81.22	90.88	92.40	99.35	102.96	19.67	
c	342.0	87.0	86.66	80.55	85.33	95.17	95.44	102.12	105.50	19.79	
	Run 79, $m/M = 1.00$										
k	344.5	89.5	89.23	83.26	87.50	99.09	98.44	105.09	108.34	19.99	
l	344.3	92.8	92.53	86.79	95.57	103.60	102.15	108.56	111.64	19.71	
n	344.3	101.6	101.25	96.23	100.33	113.85	111.89	117.84	120.64	19.54	
o	344.4	132.0	131.86	128.09	138.55	144.66	143.85	148.47	150.67	18.27	
p	344.2	158.7	158.56	155.60	165.59	171.32	170.62	174.43	176.32	17.43	

of flow on the assumption that the air passed through the gas meters at 70 deg F and 760 mm Hg, under which conditions a flow rate of 1 liter per min is equivalent to 0.1587 lb per hr.

The efficiency η corresponding to each setting of the outlet pressure P_3 was computed from equation (1), using enthalpies obtained from the gas tables of Keenan and Kaye [7]. The enthalpies h_1 and h_2 remain constant at 126.66 Btu per lb in consequence of the assumption that the inlet air was always at 530 F abs. Data selected from three typical runs are given in Table 1, and in Fig. 4 the efficiencies found in these runs are plotted against the outlet pressure P_3 . About half the experimental data have been omitted from Table 1, but the plotted points in Fig. 4 represent all the data taken in the three runs. As the outlet pressure P_3 is increased, the efficiency first rises, then passes through a maximum, and finally decreases. The height of the maximum and the general shape of the curve clearly depend on the entrainment ratio. In a run such as those shown in Fig. 4, a change in P_3 is accompanied, in general, by changes in all the other observed pressures except P_1 . Since the flow at the throat of the driving-fluid nozzle is sonic, changes in conditions downstream from the

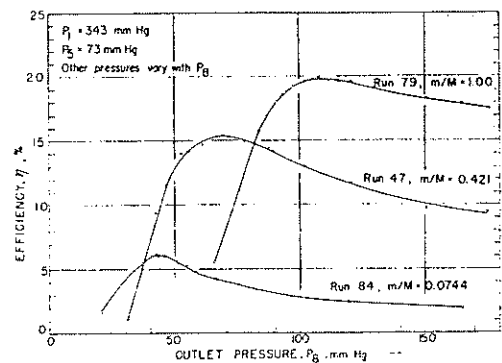


Fig. 4 Efficiency versus outlet pressure for three typical runs

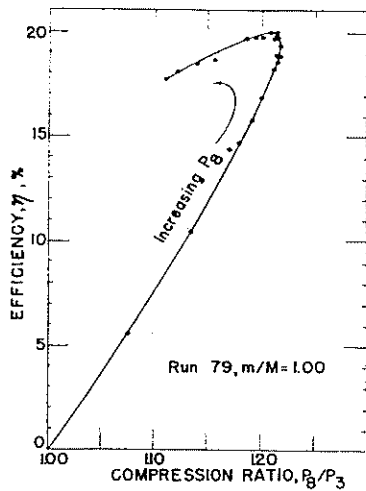


Fig. 5 Efficiency versus compression ratio for a typical run

throat cannot affect P_1 , which remains substantially constant throughout a run.

Many investigators have analyzed their data using the compression ratio, P_2/P_3 , as an independent variable where we have used the outlet pressure P_2 . Fig. 5 shows how one of the curves (run 79) of Fig. 4 is transformed when compression ratio is used as the abscissa instead of outlet pressure. The high-pressure arm of the original curve is folded over and lies above the low-pressure arm. Hence there are in general two different modes of operation corresponding to the same compression ratio, and the mode in which both P_2 and P_3 are larger gives the higher efficiency. It has sometimes been assumed that, for a given entrainment ratio, maximum efficiency is synonymous with maximum compression ratio. A look at equation (1) shows that this is only approximately true. The maximum value of $h_2 - h_3$ will occur when P_2/P_3 is maximum and if, changes in the denominator of equation (1) are negligible, maximum efficiency will coincide with maximum compression ratio. However, changes in the denominator cannot be entirely neglected. As P_2 increases, h_{10} increases and the denominator decreases. This displaces the point of maximum efficiency to a higher value of P_2 than that corresponding to maximum compression ratio. For example, in run 79 the maximum compression ratio (P_2/P_3) occurred at $P_2 = 97$ mm Hg whereas the maximum efficiency occurred at $P_2 = 108.0$ mm Hg.

To find the relation between entrainment ratio and efficiency, a large number of runs was made and the results plotted in the manner of Fig. 4. The maximum efficiency was then read from each curve and recorded. The maximum efficiencies thus found are given in Table 2, together with the values of P_2 and other important parameters that correspond to the maximum value of η .

For most of the data in Table 2, M is approximately equal to 1.587 lb per hr (10 l per min). All the data for which M has this value are represented in Fig. 6, in which maximum efficiency is plotted against entrainment ratio. Starting at zero with zero entrainment, the curve rises to a maximum efficiency of 20.6 per cent at an entrainment ratio of about 1.3 and then starts to fall. The last part of the curve is dotted, to indicate a rapid decrease in accuracy above an entrainment ratio of about 1.35.

Efficiency curves such as those shown in Fig. 4 sometimes showed irregularities, which often took the form of sharp drops in efficiency covering a range in P_2 of 5 to 10 mm Hg. These irregularities were at first attributed to experimental error, but later it was found that in many cases they were highly reproducible.

Table 2 Conditions of efficiency maxima

The values of η_{max} were determined from the curves of Fig. 4 and from similar plotted curves for all the other runs. Data in the table refer to conditions at these maxima.

Run	P_1 mm Hg	P_2 mm Hg	P_3 mm Hg	P_2/P_1	P_2/P_3	M lb/hr	m/M	η_{max} %	P_2/P_3
59	344.0	17.0	48.0	0.1395	2.820	1.59	0.0559	4.30	0.23
86	340.0	15.4	45.0	0.1324	2.915	1.57	0.0764	6.15	0.21
58	346.8	17.0	45.0	0.1325	2.700	1.59	0.0851	6.40	0.22
52	342.5	16.4	44.0	0.1285	2.680	1.56	0.104	7.61	0.23
57	346.7	18.0	47.5	0.1370	2.638	1.59	0.115	6.60	0.24
63	342.0	19.7	47.0	0.1374	2.385	1.58	0.161	10.60	0.28
56	347.0	25.2	55.0	0.1585	2.180	1.59	0.190	11.60	0.31
62	346.0	24.1	48.0	0.1387	1.995	1.59	0.241	12.30	0.31
45	346.5	32.8	60.0	0.1732	1.828	1.57	0.294	14.05	0.41
46	346.0	38.5	64.0	0.1850	1.662	1.58	0.361	14.80	0.50
47	343.8	43.8	68.0	0.2978	1.553	1.57	0.421	15.30	0.56
49	344.8	50.7	76.0	0.2204	1.498	1.58	0.495	17.30	0.65
87	343.1	53.3	77.0	0.2244	1.445	1.58	0.533	17.77	0.68
50	342.5	58.0	81.0	0.2365	1.377	1.57	0.620	18.40	0.76
78	345.2	71.5	92.0	0.2665	1.287	1.58	0.806	19.10	0.90
79	344.5	89.2	108.0	0.3135	1.211	1.58	1.00	19.90	1.13
80	336.9	109.3	122.0	0.3621	1.159	1.58	1.20	20.50	1.16
86	331.0	106.9	122.0	0.3664	1.141	1.56	1.32	20.50	1.40
85	317.0	106.5	123.0	0.3590	1.136	1.56	1.40	20.55	1.39
81	336.9	111.0	124.0	0.3681	1.117	1.57	1.52	19.60	1.39
82	345.2	114.9	124.0	0.3592	1.079	1.58	1.83	15.80	1.34
69	515.8	15.5	56.5	0.1095	3.645	2.38	0	0	0.15
64	402.8	32.9	64.0	0.1589	1.943	1.84	0.277	14.20	0.35
72	346.5	49.5	74.0	0.2136	1.495	1.59	0.485	16.65	0.62
73	304.0	58.7	78.0	0.2566	1.328	1.40	0.681	17.90	0.85
77	255.8	68.8	81.5	0.3186	1.185	1.18	1.01	18.00	1.17

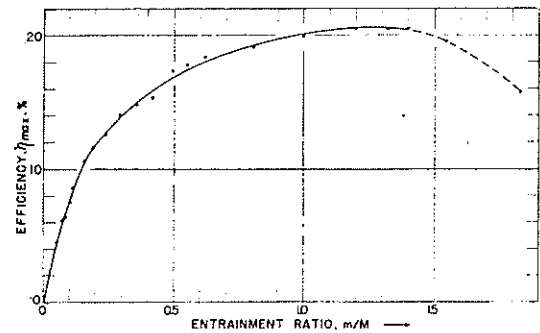


Fig. 6 Maximum efficiency versus entrainment ratio

Further study will be required to establish their cause. It is believed that the accuracy of Fig. 6 is not seriously affected by the existence of these irregularities.

The relationship between the pressures of the driving and the driven streams as they come in contact is a matter of considerable interest. If the driving fluid has a higher pressure than the driven stream it is said to be underexpanded. Conversely, the condition in which the driving stream has the lower pressure is referred to as overexpansion. Royds and Johnson [4] suggest that an air ejector should be operated with a moderate amount of underexpansion. In the discussion on their paper, and elsewhere in the literature, a number of opinions on this question are expressed. Our data give an experimental answer to this problem. The pressure P_2 of the driving fluid as it leaves the driving-fluid nozzle cannot be directly measured in our apparatus. However, if a reasonable value of nozzle efficiency is accepted, this pressure can be calculated with an error that probably does not exceed 10 per cent. Such a calculation has been made, using methods described later in this paper, where the plotting of points on the h - s diagram is described. The pressure P_2 is the pressure of the driven fluid when it first comes in contact with the driving fluid. Contact occurs at a point somewhere between the two pressure taps c and d , Fig. 2. The pressure P_d at tap d , the first tap on the mixing tube, was taken to be P_2 . This procedure requires some justification. Reference to Table 1 shows that P_d was always somewhat lower than P_2 . The percentage difference in the neighborhood of maximum efficiency was 3.4 for run 84, 5.3 for

run 47, and 6.7 for run 79. Hence within an error of 10 per cent or less, the pressure at either tap can be taken to represent P_6 . It is not considered possible that a pressure widely different from P_6 or P_4 could exist between the two taps because the flow of driven fluid was always subsonic in this region.

For each point of maximum efficiency in Table 2, the pressure ratio P_6/P_5 has been computed and included in the table. When this ratio is plotted against the entrainment ratio m/M , the curve of Fig. 7 is obtained. The value of P_6/P_5 at maximum efficiency increases with m/M . Within the experimental error the relation is linear up to $m/M = 1.0$. In this region P_6/P_5 appears to rise slightly above the straight line. Near $m/M = 1.2$ the curve levels out and appears to diminish slightly at the highest entrainment ratios investigated. The linear portion of the graph in Fig. 7 does not pass through the origin but it comes rather near it. Now a straight line passing through the origin of Fig. 7 corresponds to a simple variation of conditions inside the jet compressor. With P_5 and M held constant (this was the case with Fig. 7) a straight line through the origin corresponds to the acceptance of a constant volume-rate of flow of driven fluid. Under such circumstances, when the entrainment ratio is increased both the pressure and the density of the driven fluid increase in proportion, and there is no change in the velocity of the driven fluid. This picture does not exactly correspond to the situation shown in Fig. 7 but it is not a bad approximation for a considerable range of m/M .

At an entrainment ratio of approximately 0.88, P_6/P_5 reaches the value 1. For all lower entrainment ratios, maximum efficiency requires the driving fluid to be underexpanded ($P_6/P_5 < 1$). Conversely, if the entrainment ratio is greater than 0.88, overexpansion of the driving fluid ($P_6/P_5 > 1$) is required for maximum efficiency. These results refer, of course, only to the apparatus used in the present experiments. One would expect that, if another apparatus were used, a curve of the same general shape as Fig. 6 would be obtained, but it would not necessarily pass through the same numerical values. It must also be borne in mind that both P_6 and P_5 are uncertain by perhaps 10 per cent, so that the ordinates in Fig. 7 are uncertain by 15 or 20 per cent. The internal consistency is much better than this figure, of course.

In the theory of constant-pressure mixing, the driving and driven streams are assumed to be at the same constant pressure from the moment of contact until mixing is complete. In Fig. 7, constant-pressure mixing is probably approximated most closely when $P_6/P_5 = 1$, since in this case the assumed conditions are at least satisfied as mixing begins. The efficiency maxima of runs 84, 47, and 79 were compared with Fig. 11 of Keenan, Neumann, and Lustwerk [1], which is based on the theory of constant pressure mixing. Using the experimentally observed abscissa (our P_1/P_2) and the curve corresponding to our area-ratio ($=9.93$) the ordinate (P_6/P_5 in our notation) can be obtained and compared with the experimentally observed value.

The results of the comparison are as follows:

Run	84	47	79
m/M	0.0744	0.421	1.00
A_7/A^*	9.93	9.93	9.93
P_1/P_2	22.021	7.851	3.863
P_6/P_5	2.915	1.553	1.211
(P_6/P_5) calc from KNL's } Fig. 11	3.7	1.9	1.3
(P_6/P_5) obs/ (P_6/P_5) calc	0.79	0.82	0.93
P_6/P_5	0.21	0.56	1.13

The agreement is slightly better near $P_6/P_5 = 1$ than elsewhere. If, instead of using the area-ratio curve of Fig. 11 of Keenan, et al., we ignore it and use the entrainment-ratio curves corresponding to experiment, the agreement between observed and calculated values of P_6/P_5 is much worse than that shown in the table above. Since our data were not taken under conditions that would provide an optimum test of either constant-pressure or

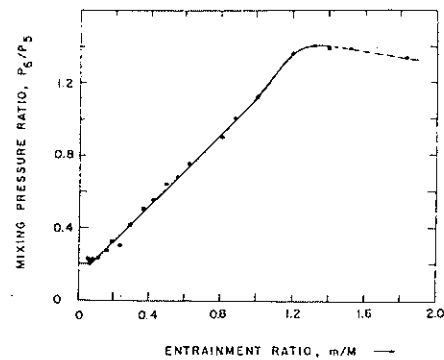


Fig. 7 Mixing pressure ratio at maximum efficiency versus entrainment ratio

constant-area mixing, a full-scale comparison with these theories has not been included in this paper.

Plotting Experimental Data on the h - s Diagram

A few typical sets of observations from the experimental data have been plotted to scale in the h - s diagram of Fig. 3. The condition lines are helpful in visualizing various parts of the compression process, and the increases in entropy indicate where the major losses occur. The data plotted in Fig. 3 are observations 79a, 79k, and 79p, all from Table 1. Referring to Fig. 4, one observation corresponds to a point near the maximum of the efficiency curve, and the other two correspond to points near the two ends. The condition line 1-5 represents passage of the driving fluid through its nozzle and is the same for all the observations. The mixing process cannot be represented in the diagram. Three arrows point from state 5 to the three states 7, indicating that after mixing is complete the mixed stream is in state 7. The points 7 correspond to pressure tap f. The three states 3 represent the initial condition of the driven fluid. Arrows indicate that during the mixing process the driven fluid is transferred to the appropriate state 7. A part of the path from 3 to 7 (3-6) can be plotted if the necessary data (pressures and cross-section areas) are available. The paths 3-6 have not been plotted to scale in Fig. 3 but for one observation (79k) the path is shown schematically. The three lines 7-8 represent states along the path of deceleration and compression of the mixed stream between the last tap on the mixing tube and the outlet. These lines all show a small over-all increase of entropy in the direction of flow, as they should. The fact that the curves exhibit a few decreases of entropy between successive experimental points must be attributed to the cumulation of errors in the flow rates, cross section, and observed pressures. Fig. 3 shows clearly that the large entropy increases, and hence the large losses, are associated with the mixing process. This conclusion comes as no surprise, of course.

The method by which points on the condition lines may be located on the h - s diagram will be briefly described. There is, of course, no trouble with the points 1, 3, and 8. In these states the fluid is at rest, and measurements of pressure and temperature permit the enthalpy and entropy to be determined from the Gas Tables [7]. The pressures of these states were measured and the temperatures were assumed always to be 530 F abs (70 F). Hence $h_1 = h_3 = h_8 = 126.66$ Btu per lb. The assumption that T_2 is the same as T_1 and T_4 is easily justified by the law of conservation of energy, provided heat transfer to or from the gas within the apparatus is negligible, and provided it is permissible to treat h as a function of temperature only. These conditions were adequately satisfied in the present experiments.

The points representing states in which the fluids are in motion may be located with the aid of Fanno lines. Using the equations

of energy and continuity, the ideal gas law, and the approximation $h_1 - h = c_p(T_1 - T)$, the equation of a Fanno line may be put in the form

$$T = \frac{c_p P^2}{G^2 R^2} \left[-1 + \left(1 + 2T_1 \frac{G^2 R^2}{c_p P^2} \right)^{1/2} \right] \quad (2)$$

where G is the mass flow rate per unit of cross section area and T_1 is the temperature of the fluid when at rest. Since the mass flow rates m and M are known G can be computed for any point at which the cross section has been measured (cf table of dimensions). Substituting observed values of P into equation (2), T is obtained. All other thermodynamic properties may then be obtained from the Gas Tables [7].

This procedure was used for the points on the condition lines 7-8 using $T_1 = T_8 = 530$ F abs. Unfortunately it could not be used for the point 5. The pressure at point 5 (driving-nozzle exit) is of particular interest because it is at this point that the driving and driven streams first come in contact. The nature of the apparatus did not permit P_5 to be experimentally observed, so it was necessary to compute P_5 on the basis of some reasonable assumption regarding losses. The losses were assumed to be negligible in the subsonic part of the nozzle and to be 10 per cent in the supersonic part. By trial it was found that a temperature drop from 530 to 441.5 F abs was sufficient to impart sonic velocity to air at the lower temperature. The temperature and enthalpy at the throat are $T^* = 441.5$ F abs and $h^* = 105.47$ Btu per lb. The velocity of sound at this temperature [8] is 1030 ft per sec and the pressure $P^* = 0.528P_1$ with the assumption of no losses. Referring to Fig. 3, the assumption of 90 per cent efficiency in the supersonic region of the nozzle requires that point 5 should satisfy the condition $h^* - h_5 = 0.90(h^* - h_2)$ where point 2 lies on the isentropic through point 1 and the constant-pressure line through point 5. Using equation (2) it was found by trial that the condition was satisfied when $T_5 = 350.3$ F abs, $h_5 = 83.64$ Btu per lb, and $P_5/P_1 = 0.213$. These values are independent of P_1 under the assumed conditions and to the accuracy of the gas tables used. The velocity at point 5 is found from the enthalpy drop to be 1468 ft per sec. The velocity of sound in air at $T_5 = 350.3$ F abs is 918 ft per sec [8]. Hence the Mach number is 1.60 if the assumed losses are correct.

Conclusions

The results presented in the present paper show how the con-

dition of maximum operating efficiency of a jet compressor may be found, when entrainment ratio and outlet pressure are varied. The changes in these two variables automatically introduce changes in many other variables, including the initial pressure of the driven fluid and the compression ratio. However, some of the important parameters could not be varied because of the nature of the apparatus, and others that could have been varied have so far been held constant by choice. The variables that we have thus far not fully investigated include the expansion ratio of the driving fluid, the position of the driving-fluid nozzle, the temperatures of the input streams, the geometry of the inlet, diffuser, and other parts of the apparatus, and the molecular-weight ratio of the driving and driven fluids. These facts leave plenty of reason to hope that efficiencies substantially above 20.6 per cent (which is the highest value now being reported) are not out of the question. Present plans call for systematic study of the variables thus far not investigated.

Acknowledgment

The authors wish to acknowledge valuable consultations with Prof. Joseph Kaye of the Massachusetts Institute of Technology during the course of this research.

References

- 1 J. H. Keenan, E. P. Neumann, and F. Lustwerk, "An Investigation of Ejector Design by Analysis and Experiment," *Journal of Applied Mechanics*, vol. 17, TRANS. ASME, vol. 72, 1950, pp. 299-309.
- 2 J. H. Keenan and E. P. Neumann, "A Simple Air Ejector," *Journal of Applied Mechanics*, vol. 9, TRANS. ASME, vol. 64, 1942, pp. A-75-81.
- 3 L. J. Kastner and J. R. Spooner, "An Investigation of the Performance and Design of the Air Ejector Employing Low-Pressure Air as the Driving Fluid," *Proceedings of the Institution of Mechanical Engineers*, vol. 162, 1950, pp. 149-159. Discussion, *ibid.*, pp. 160-166.
- 4 R. Royds and E. Johnson, "The Fundamental Principles of the Steam Ejector," *Proceedings of the Institution of Mechanical Engineers*, vol. 145, 1941, pp. 193-209. Discussion, *ibid.*, vol. 146, 1942, pp. 223-235.
- 5 G. Flügel, "The Design of Jet Pumps," National Advisory Committee for Aeronautics, TM 982, 1941, translated from VDI Forschungsheft 395, 1939.
- 6 J. H. Keenan, "Thermodynamics," John Wiley & Sons, New York, N. Y., 1941, p. 155.
- 7 J. H. Keenan and J. Kaye, "Gas Tables," John Wiley & Sons, New York, N. Y., 1948. Table 1 of this collection was used.
- 8 J. Hilsenrath, et al., "Tables of Thermal Properties of Gases," National Bureau of Standards Circular 564, 1955, p. 63.